Molecular Pharmacology Fast Forward. Published on December 14, 2006 as doi:10.1124/mol.106.030031

MOL30031

Activation of the CXCR3 chemokine receptor through anchoring of a small molecule chelator ligand between TM-III, -IV and -VI

Mette M.Rosenkilde[1], Michael B.Andersen, Rie Nygaard, Thomas M.Frimurer[1] & Thue W.Schwartz[1]

Laboratory for Molecular Pharmacology, Department of Pharmacology,

University of Copenhagen, Copenhagen, DK-2200, Denmark (MMR, MBA, RN, TWS)

& 7TM Pharma A/S, Hørsholm, DK-2970, Denmark (RN, TMF, TWS)

Molecular Pharmacology Fast Forward. Published on December 14, 2006 as DOI: 10.1124/mol.106.030031
This article has not been copyedited and formatted. The final version may differ from this version.

MOL30031

Running title: 7TM activation by metal-ion site anchored chelator

Editorial correspondence:
Thue W.Schwartz
Laboratory for Molecular Pharmacology,
Department of Pharmacology, The Panum Institute
University of Copenhagen
Blegdamsvej 3b, DK-2200, Copenhagen, Denmark
Email: Schwartz@molpharm.dk
Phone: +45 2262 2225; Fax: +45 3532 7610

Text pages: 32
Tables: 3
Figures: 8
References: 42
Words in abstract: 250
Words in Introduction: 634
Words in Discussion: 1944
Supplementary data: 7 pages

List of non-standard abbreviations: CXCR3 – chemokine CXC receptor type 3; IP10 – chemokine CXC ligand 10; ITAC – chemokine CXC ligand 11; NOE – Nuclear Overhauser effect; RMSD – root mean square deviation; TM – transmembrane segment.

Molecular Pharmacology Fast Forward. Published on December 14, 2006 as DOI: 10.1124/mol.106.030031
This article has not been copyedited and formatted. The final version may differ from this version.

Abstract

7TM receptors are activated through a common, still rather unclear molecular mechanism by a variety of chemical messengers ranging from monoamines to large proteins. By introducing a His residue at position III:05 in the CXCR3 receptor a metal-ion site was built between the extracellular ends of TM-III and TM-IV to anchor aromatic chelators at a location corresponding to the presumed binding pocket for adrenergic receptor agonists. In this construct free metal-ions had no agonistic effect in accordance with the optimal geometry of the metal-ion site in molecular models built over the inactive form of rhodopsin. In contrast, the aromatic chelators bipyridine or phenanthroline in complex with Zn(II) or Cu(II) acted as potent agonists displaying signaling efficacies similar to or even better than the endogenous chemokine agonists. Molecular modeling and molecular simulations combined with mutational analysis indicated that the metal-ion site anchored chelators act as agonist by establishing an aromatic-aromatic, second-site interaction with TyrVI:16 on the inner face of TM-VI. Importantly, this interaction required that the extracellular segment of TM-VI moves inward in the direction of TM-III, whereby TyrVI:16 together with the chelators complete an “aromatic zipper” also comprising PheIII:08 – corresponding to the monoamine receptor anchoring point – and TyrVII:10 - corresponding to the retinal attachment site in rhodopsin. Chemokine agonism was independent of this aromatic zipper. It is proposed that in rhodopsin-like 7TM receptors small molecule compounds in general act as agonists in a similar manner as here demonstrated with the artificial, metal-ion site anchored chelators, by holding TM-VI bent inward.

Molecular Pharmacology Fast Forward. Published on December 14, 2006 as DOI: 10.1124/mol.106.030031
This article has not been copyedited and formatted. The final version may differ from this version.

Introduction

7TM (seven transmembrane segment) or G-protein coupled receptors constitute the largest family of proteins in the human genome being activated by a very broad variety of chemical messengers, odor and taste components: from calcium-ions to large glycoprotein hormones over all kinds of small molecules such as monoamines, amino acids, purines, lipids, neuropeptides as well as larger peptide hormones and small proteins such as chemokines (Bockaert and Pin, 1999;Lefkowitz, 2004).

Several X-ray structures have been generated for rhodopsin, but they all represent the same inactive, dark state of the molecule (Palczewski et al., 2000;Okada et al., 2004;Li et al., 2004). Even the structure of metarhodopsin-I, in which the inverse agonist 11-cis retinal is converted to the all-trans, agonist form, has a very similar overall protein structure as compared to the inactive state of the protein (Ruprecht *et al.*, 2004). It is, however, known from a number of biochemical and biophysical studies that major conformational changes occur in the receptor protein during the subsequent transformation into the active, signaling metarhodopsin-II form (Hubbell et al., 2003;Sakmar et al., 2002). In particular the comprehensive, site-directed spin labeling studies by Hubbell and Khorana and coworkers have shown that during activation the intracellular segments of the transmembrane helices – especially TM-VI – undergo relatively large-amplitude rigid-body movements away from each other and thereby reveal activating receptor epitopes for down-stream signaling molecules (Farrens *et al.*, 1996;Hubbell *et al.*, 2003). A number of biochemical and biophysical studies especially in the β2-adrenergic receptor support this picture (Gether *et al.*, 1997;Ballesteros *et al.*, 2001).

Only rather limited information is available concerning movements of the extracellular segments of the TMs. However, based on the distance constraints imposed by a number of activating metal-ion sites constructed between TM-III, -VI and –VII, we recently

Molecular Pharmacology Fast Forward. Published on December 14, 2006 as DOI: 10.1124/mol.106.030031
This article has not been copyedited and formatted. The final version may differ from this version.

proposed a Global Toggle Switch activation model for 7TM receptors (Elling *et al.*, 2006). According to this model, an inward movement of the extracellular segments – especially TM-VI and TM-VII – was suggested to be coupled to the well established outward movement of the intracellular segments of these helices. The conserved proline-bends of the involved helices appear to constitute the pivots for these vertical see-saw movements (Elling *et al.*, 2006). Such a model, with a considerable induced-fit component comprising a "closing" of the binding-pocket around the small agonist ligand, is in agreement with recent structure-function studies in both the β2-adrenergic receptor and the M3 muscarinic receptor (Carmine R.D. et al., 2004;Swaminath et al., 2004;Kobilka, 2004;Liapakis et al., 2004;Han et al., 2005).

In the present study we test the hypothesis that small molecules act as agonists for 7TM receptors by holding TM-VI and –VII in an inwardly-bent, proposed active conformation. An engineered metal-ion site is employed as an anchor point to tether small, aromatic chelators in the main ligand-binding pocket of the CXCR3 chemokine receptor (Fig. 1) at a position corresponding to the presumed binding site for catecholamine agonists in, for example, the β2-adrenergic receptor (Kobilka, 2004;Shi and Javitch, 2002). The CXCR3 receptor, which normally is activated by large chemokines such as ITAC (CXCL11) and IP10 (CXCL10), was chosen as a model system because it has previously proven to be particularly robust and well suited for extensive mutational engineering in the main ligand-binding pocket (Rosenkilde *et al.*, 2004). Through mutational analysis combined with molecular modeling and simulations it is found that the metal-ion site anchored chelators act as highly efficacious agonists through establishing second-site, aromatic-aromatic interactions with a Tyr residue on the inner face of TM-VI, TyrVI:16, and thereby completing an "aromatic zipper" between TM-III, -VI, and –VII, which holds the extracellular segment of especially TM-VI in an inwardly-bent, presumed active

Molecular Pharmacology Fast Forward. Published on December 14, 2006 as DOI: 10.1124/mol.106.030031
This article has not been copyedited and formatted. The final version may differ from this version.

conformation. The two other components of the proposed aromatic zipper TyrIII:08 and TyrVII:10 are located at the classical anchor-point for monoamines (AspIII:08 in monoamine receptors) and the attachment site for retinal in TM-VII, LysVII:10 (Lys^{296}) in rhodopsin, respectively.

MATERIAL AND METHODS

Materials. The CXCR3 chemokine ligands CXCL10/IP10 and CXCL11/ITAC were purchased from Peprotech. The metal-ion chelator complexes were created by mixing 2,2'-bipyridine (Aldrich) or 1,10-Phenanthroline with $CuCl_2$ or $ZnCl_2$ in the relation 2:1. Human CXCR3 cDNA was kindly provided by Kuldeep Neote (Pfizer, CT). The Gα6qi4myr construct was kindly provided by Evi Kostenis (Bonn, Germany).

Site-directed Mutagenesis. Point mutations were introduced in the receptors by the polymerase chain reaction overlap extension technique. All reactions were carried out using the *Pfu* polymerase (Stratagene) under conditions recommended by the manufacturer. The generated mutations were cloned into the eukaryotic expression vector pcDNA3+. The mutations were verified by DNA sequencing (MWG Biotech).

Transfections and cell culture. COS-7 cells were grown at 10% CO_2 and 37ºC in Dulbecco's modified Eagle's medium with glutamax (Gibco) adjusted with 10% fetal bovine serum, 180 u/ml penicillin and 45 ug/mL streptomycin. Transfection of the COS-7 cells was performed by the calcium phosphate precipitation method (Rosenkilde *et al.*, 1999).

Phosphatidyl-inositol assay (PI-turnover). COS-7 cells (6 x 10^6 cells/flask) were transfected with 20 μg receptor cDNA in addition to 30 μg of the promiscuous chimeric G-protein, Gα6qi4myr (Kostenis *et al.*, 1998) , which turns the Gαi coupled signaling of

Molecular Pharmacology Fast Forward. Published on December 14, 2006 as DOI: 10.1124/mol.106.030031
This article has not been copyedited and formatted. The final version may differ from this version.

the CXCR3 receptor into the Gαq pathway, i.e phospholipase C activation measured as PI-turnover (Berridge *et al.*, 1983). One day after transfection, the cells were seeded into wells (2.5 x 10^4 cells/well) and incubated for 24 hours with 2 μCi of ^{3}H-*myo*-inositol (Amersham Pharmacia Biotech) in 0.4 ml growth medium per well. Cells were washed twice in 20 mM Hepes, pH 7.4, supplemented with 140 mM NaCl, 5 mM KCl, 1 mM $MgSO_4$, 1 mM $CaCl_2$, 10 mM glucose and 0.05% (w/v) bovine serum albumin; and were incubated in 0.4 ml buffer supplemented with 10 mM LiCl at 37ºC for 90 minutes in the presence of ligands. Cells were extracted by addition of 1 ml 10 mM Formic acid to each well followed by incubation on ice for 30 min. The generated [^{3}H]-inositol phosphates were purified on AG 1-X8 anion-exchange resin (Bio-Rad Laboratories) (Rosenkilde *et al.*, 1999). Determinations were made in duplicates.

Calculations. EC_{50} and potency values were determined by nonlinear regression using the GraphPad-Prism 3.0 software.

Molecular modeling and simulations. Molecular homology models of the [HisIII:05]CXCR3 re ceptor were built over the X-ray structure of the inactive state of rhodopsin using the software package MODELLER as described in detail in the supplementary material. Relibase (Hendlich *et al.*, 2003), a database of high resolution experimental protein-ligand complexes was used to design a silent, anchoring metal-ion site between a His residue introduced at position III:05 (Gly^{128} to His) and the natural Asp residue at position IV:20 (Asp^{186}). A Zn(II) metal-ion as well as an aromatic metal-ion chelator – i.e. bipyridine or phenanthroline – were docked into the molecular model which was subjected to energy minimizations. Models of the presumed active receptor conformation were generated by a Monte Carlo simulation annealing protocol (Li and Scheraga, 1987) using the NOE functionality of CHARMM with distance constraints for the extracellular segments of TM-III, TM-VI and TM-VII corresponding to Cβ-Cβ

Molecular Pharmacology Fast Forward. Published on December 14, 2006 as DOI: 10.1124/mol.106.030031
This article has not been copyedited and formatted. The final version may differ from this version.

distances defined by the previously described activating metal-ion site originally constructed between positions III:08, VI:20, and VII:06 in the β2-adrenergic receptor (Elling *et al.*, 2006) as well as distance constraints of the intracellular segments of these helices as defined by the EPR analysis of the movements in rhodopsin during activation (Hubbell *et al.*, 2003) as described in detail in the supplementary material.

RESULTS

Construction of an anchoring metal-ion site between TM-III and -IV

In the β2-adrenergic receptor the monoamine agonists use an Asp in position III:08 as a counter-ion, attachment point (Strader et al., 1991;Kobilka, 2004;Shi and Javitch, 2002). In the CXCR3 receptor we chose position III:05 (residue number 128) one helical turn "above" III:08 as the starting point for the construction of an anchoring metal-ion site (Figs. 1 and 2A). Computational chemistry analysis of the geometry of a large number of experimentally characterized metal-ion sites compiled in Relibase® (Hendlich *et al.*, 2003) revealed that a His residue introduced at this position could make a perfect metal-ion site i.e. in respect of angles and distances with the naturally occurring AspIV:20 (Asp^{186}) located on the opposing face of TM-IV with both residues in their preferred rotameric states (see supporting online material) (Fig. 1B). Position IV:20 is known to be readily accessible for small molecule non-peptide ligand interactions, as extensively studied in both the CXCR3 and CXCR4 receptors (Gerlach *et al.*, 2003;Rosenkilde *et al.*, 2004).

In accordance with the fact that HisIII:05 and AspIV:20 can form the metal-ion site already in the inactive receptor conformation, the free metal-ions, Zn(II) or Cu(II), had no agonistic effect in the [HisIII:05]-CXCR3 construct (Fig. 2B, Table 1). Similarly, the

Molecular Pharmacology Fast Forward. Published on December 14, 2006 as DOI: 10.1124/mol.106.030031
This article has not been copyedited and formatted. The final version may differ from this version.

chelators bipyridine and phenanthroline had no agonistic property on their own; neither in the wild-type nor in the [HisIII:05]-CXCR3 construct (Fig. 2C, Table 1). Importantly, when presented in complex with metal-ions, the aromatic chelators acted as high potency and high efficacy agonists in the [HisIII:05]-CXCR3 construct (Fig. 2D, Table 1). Highest potency (8.0 μM) was displayed by Cu(II)-phenanthroline, corresponding to a 38-fold increase as compared to the wild-type receptor (Table 1). In the [HisIII:05]-CXCR3 construct the endogenous chemokines ITAC and IP10 displayed an Emax which was ~ 40 % of that obtained in the wild-type CXCR3 receptor, whereas in the [HisIII:05]-CXCR3 construct the maximal efficacy of the metal-ion complexes was 1.5 to 1.8 fold *superior* to that of even the most efficacious endogenous chemokine, ITAC (CXCL11) as shown for Cu(II)-bipyridine in Fig. 3A (Table 1). No potentiating or inhibitory effect was observed during co-administration of ITAC and Cu(II)bipyridine but instead an additive effect where administration of Cu(II)bipyridine simply brought the signaling efficacy of the [HisIII:05]-CXCR3 construct up to the higher Emax observed for Cu(II)bipyridine alone (Fig. 3B and C). It can be argued that this supports a model where ITAC and Cu(II)bipyridine function as co-agonists in a non-classical type of allosteric mechanism (Schwartz and Holst, 2006).

Ala-substitution of AspIV:20 confirmed that this residue was indeed the metal-ion binding partner for HisIII:05 in the [HisIII:05]-CXCR3 construct as reflected in the 40-fold rightward shift in the dose-response curve for Cu(II)-bipyridine (Fig. 2E, Tabel 2). As a control, AspVI:23 could be mutated without any effect of the agonist potency of Cu(II)-bipyridine (Fig. 2E).

Identification of second-site interactions for the aromatic chelators

The high efficacy and potency of the metal-ion chelator complexes as compared to the free metal-ions indicate that the chelators make significant second-site interactions in the

Molecular Pharmacology Fast Forward. Published on December 14, 2006 as DOI: 10.1124/mol.106.030031
This article has not been copyedited and formatted. The final version may differ from this version.

active receptor conformation. In order to identify such interaction points, we performed a systematic mutational analysis of possible interaction partners at the inner faces of TM-III, -V, -VI, and -VII in the [HisIII:05]-CXCR3 background (Fig. 4, Tables 2 and 3). No effect was observed by substitution of the potential cation-π interaction partners ArgV:01, ArgV:05, and LysVII:02 (Fig. 4B and C, Table 2). Also, only a very minor effect was observed by Ala-substitution of the potential aromatic-aromatic interaction partners, TrpVI:13 and PheIII:12 - both located relatively deep in the pocket (Fig. 4D, Table 2). In contrast, Ala-substitution of TyrVI:16 (Tyr^{271}) shifted the dose-response curve for Cu(II)-bipyridine 37-fold to the right (Fig. 4E). Similarly, introduction of either an aliphatic, hydrophobic Leu residue or a polar Asn residue at this position impaired the potency of Cu(II)-bipyridine 58- and 31-fold, respectively (Table 2). Importantly, the potency of the chemokine ITAC was in fact *improved* 2.5- to 10-fold by these three substitutions of TyrVI:16, indicating that the mutations did not cause general harm to the receptor (Table 2). Substitution of TyrVI:16 with either a Phe or a His residue had only minor effects on the potency of Cu(II)-bipyridine (Table 2).

These results indicate that the bipyridine or phenanthroline chelators in complex with metal-ions obtain their high potency and agonist efficacy in the [HisIII:05]-CXCR3 construct though establishment of a second-site interaction with TyrVI:16 on the opposing face of TM-VI - conceivably through an aromatic-aromatic interaction.

In molecular models of the [HisIII:05]-CXCR3 receptor built over the X-ray structure of the inactive conformation of rhodopsin, even the closest distance between the bipyridine moiety tethered to HisIII:05 through the metal-ion and the side-chain of TyrVI:16 - 5.6 Å - is nevertheless too long to correspond to an aromatic-aromatic interaction. However, according to the recently proposed Global Toggle Switch activation model for 7TM

Molecular Pharmacology Fast Forward. Published on December 14, 2006 as DOI: 10.1124/mol.106.030031
This article has not been copyedited and formatted. The final version may differ from this version.

receptors, the extracellular segment of TM-VI will during activation of the receptor swing or tilt inward towards TM-III (Elling *et al.*, 2006).

Molecular simulation of the activation mechanism of [HisIII05]-CXCR3

In order to mimic the proposed vertical seesaw movements of TM-VI and TM-VII (Elling *et al.*, 2006), the molecular model of the [HisIII:05]-CXCR3 receptor was subjected to molecular simulations (se supplementary materials for details) (Fig. 5). To encourage inward movement of the extracellular segments of TM-VI and TM-VII, the Cβ-Cβ distances for the previously constructed activating metal-ion site between positions III:08, VI:16, and VII:06 in the β-2-adrenergic receptor (Elling *et al.*, 2006), were used as NOE distance constraints during the molecular simulations. Moreover, in order to make the intracellular segments of these helices move outward, the distance constraints provided by the EPR analysis of the activation mechanism for rhodopsin were applied to the intracellular segments of TM-VI and -VII (Hubbell *et al.*, 2003) (Fig. 5). The root mean square deviation (RMSD) for the trajectories was followed during the simulation. As shown in Fig. 6A, after 4.000 Monte Carlo steps the simulation converged towards a stable conformation, which had an RMSD of approx. 2 Å relative to the starting, inactive CXCR3 conformation. Similarly, the total energy of the system demonstrates a stable simulation with decreasing energies of the system which converges to a steady level half way through the simulation.

As a result of the inward movement of the extracellular segment of TM-VI during the molecular simulation, the distance between the lower ring of the bipyridine chelator and the phenol ring of TyrVI:16 shortened to ~ 3 Å, which is compatible with a close aromatic-aromatic interaction (Fig. 5C). As shown in Fig. 6A and B, during the proposed activation process the side-chain of TyrVI:16 moves into a position, where it interacts

Molecular Pharmacology Fast Forward. Published on December 14, 2006 as DOI: 10.1124/mol.106.030031
This article has not been copyedited and formatted. The final version may differ from this version.

closely not only with the lower ring of the pyridine ligand but also with the side-chain of PheIII:08 (Phe^{131}). The opposite side of PheIII:08 on the other hand interacts closely with TyrVII:10 (Tyr^{308}) (Fig. 6A and B).

Thus, the molecular modeling and simulations indicate that the aromatic metal-ion chelator from its tethered position in the bi-dentate metal-ion site between HisIII:05 and AspIV:20 acts as an agonist by establishing a second-site, aromatic-aromatic interaction with TyrVI:16, which presumably holds TM-VI in its active, inwardly bent conformation. Importantly the molecular simulations also indicates that the aromatic chelator and TyrVI:16 together with PheIII:08 and TyrVII:10 form an extended "aromatic zipper" between the extracellular segments of TM-III, TM-VI, and TM-VII.

Mutational analysis of the proposed "aromatic zipper"

Substitution of PheIII:08 in the [HisIII:05]-CXCR3 background shifted the dose-response curves for all the metal-ion chelator complexes 18- to 124-fold to the right as compared to the wild-type receptor (Fig. 7B) (Tables 2 and 3). Importantly, the PheIII:08 substitution had only a minimal (2.4-fold) effect on the potency of the endogenous chemokine (Table 2). Thus, PheIII:08 is essential for the activation of the metal-ion site engineered CXCR3 receptor by metal-ion chelator complexes, although this residue according to the molecular models is not in direct contact with the ligand (Fig. 6) [2]. Similarly, even the side-chain of TyrVII:10, which completes the proposed "aromatic zipper" at the opposite end of the main ligand-binding pocket - as compared to the bipyridine moiety - was also found to be highly important for the activation mechanism as Ala-substitution of TyrVII:10 shifted the dose-response curves for the metal-ion chelator complexes 11- to 50-100 fold to the right (Fig. 7C, Table 2). Also in the case of TyrVII:10, the dependency upon the proposed aromatic zipper was restricted to the aromatic chelators agonists and not the chemokine proteins (Table 2).

Molecular Pharmacology Fast Forward. Published on December 14, 2006 as DOI: 10.1124/mol.106.030031
This article has not been copyedited and formatted. The final version may differ from this version.

In conclusion, the mutational analysis indicates that all four components of the "aromatic zipper" across the main ligand-binding crevice are required to hold the receptor in its active conformation when activated by the small aromatic chelators. The interaction between the metal-ion site-tethered bipyridine moiety and TyrVI:16 is not in itself sufficient to stabilize the active receptor conformation as the backing of TyrVI:16 by PheIII:08 is essential (Fig. 7B). However, not even the stabilization of TyrVI:16 by PheIII:08 is enough, as indicated by the clear effect of Ala-substitution of TyrVII:10 located "behind" both TyrVI:16 and PheIII:08 (Fig. 7C). That is, these aromatic residues are required when the small aromatic chelators bipyridine or phenanthroline act as agonists. In contrast, the large chemokine proteins can activate the receptor totally independent on these residues located relatively deep in the main ligand binding pocket of the CXCR3 receptor. Moreover, the lack of appreciable constitutive activity of the CXCR3 receptor indicates that the interdigitation of the endogenous three aromatic side chains of TyrVI:16, PheIII:08, and TyrVII:10 is not strong enough to hold the receptor in its active conformation without the presence of the metal-ion site tethered aromatic chelator.

DISCUSSION

In rhodopsin-like 7TM receptors, the binding sites for small molecule ligands - agonists as well as antagonists – have repeatedly been described to be located in the main ligand-binding pocket between the extracellular segments of the seven helical bundle, with special focus on the interfaces of TM-III, -V and TM-VI, and -VII (Schwartz et al., 1995;Shi and Javitch, 2002;Schwartz and Holst, 2002). However, although various differences have been described between agonist and antagonist interactions in specific cases, the general molecular mechanism, which for some compounds leads to agonism

Molecular Pharmacology Fast Forward. Published on December 14, 2006 as DOI: 10.1124/mol.106.030031
This article has not been copyedited and formatted. The final version may differ from this version.

and for other perhaps structurally rather similar compounds instead leads to antagonism, has remained unclear. The results of the present study provides evidence for the notion that compounds, which are agonists, are those, which are able to function as “molecular glue” between the extracellular segments of TM-III, -VI and -VII in a way that stabilizes an inwardly-bent, active conformation of especially TM-VI (Fig. 5). In contrast, compounds which bind in the same pocket, but which are not able to hold TM-VI in the correct inwardly-bent conformation or even prevent this inward movement of TM-VI and –VII, will then in stead be expected to act as antagonists or inverse agonists [3].

Small molecule 7TM agonists

Residues involved in ligand binding in the β2-adrenergic receptor – a prototype 7TM receptor - have been identified and studied extensively over the last approx. 15 years (Shi and Javitch, 2002;Kobilka, 2004;Strader et al., 1991) (Fig. 8a). The key anchoring site for agonists in the β2-adrenergic receptor - as well as in all other monoamine receptors - is the highly conserved AspIII:08, which functions as a counter-ion for the positively charged amine group of the ligand (Shi and Javitch, 2002;Strader et al., 1991). One way to envision the agonist induced activation process in this receptor would be, that a compound such as isoproterenol initially is tethered through long-range, charge-charge interactions with AspIII:08 and is oriented in the binding pocket by hydrogen-bond interactions between the cathechol ring and serine residues in TM-V to subsequently make the final, critical interactions with residues on the inner faces of TM-VI, in particular AsnVI:20 and PheVI:17 (Shi and Javitch, 2002;Kobilka, 2004;Strader et al., 1991;Wieland et al., 1996;Carmine R.D. et al., 2004;Liapakis et al., 2004) (Fig. 5A). It has recently been proposed that the binding and activation process in the β2-adrenergic receptor has to involved a certain amount of induced fit (Liapakis et al., 2004;Kobilka,

Molecular Pharmacology Fast Forward. Published on December 14, 2006 as DOI: 10.1124/mol.106.030031
This article has not been copyedited and formatted. The final version may differ from this version.

2004;Carmine R.D. et al., 2004). However, although isoproterenol is a relatively small agonist it is still difficult to precisely predict its mode of action. For example, the relative contribution of the various potential hydrogen bond donor/acceptor residues in TM-IV and V as well as the aromatic residues in TM-VI is still somewhat unclear. In the present study we have addressed the question of mechanism of action for small molecule agonists by instead making a small, very simple organic compound – bipyridine or phenanthroline – act as a highly efficacious agonist by tethering it through an anchoring, silent metal-ion site at a position corresponding to the β2-adrenergic agonists binding site between TM-III and V in a receptor, which normally is activated by large chemokines (Fig. 8). The molecular modeling and simulations as well as mutational analysis indicate that the small aromatic chelators act as agonists by establishing an aromatic-aromatic second site interactions with TyrVI:16 on the opposing face of TM-VI (Figs. 5,6). Importantly, this aromatic-aromatic interaction can only be established if the extracellular segment of TM-VI is tilted inward to a position defined by the distance constraints identified by the activating metal-ion sites previously built between positions III:08, VI:16 and VII:06 in the β2-adrenergic receptor (Elling *et al.*, 2006). Interestingly, in the metal-ion site engineered CXCR3 receptor the chelator and TyrVI:16 form part of an extended aromatic zipper also comprising PheIII:08, which corresponds to the monoamine anchor point, as well as TyrVII:10, which corresponds to the Schiff-base attachment site for retinal in TM-VII of rhodopsin, i.e. LysVII:10 (Lys^{296}). Not only TyrVI:16 but also PheIII:08 as well as TyrVII:10 are required for the agonist action of the aromatic chelators i.e. to hold TM-VI and -VII in an inwardly bent, active conformation (Fig. 3).

These observations also illustrate, that in ligand-receptor interactions it is not only the residues in direct contact with the ligand that are important. Clearly, second row or even third row residues can - in an indirect manner - be essential in establishing the binding

Molecular Pharmacology Fast Forward. Published on December 14, 2006 as DOI: 10.1124/mol.106.030031
This article has not been copyedited and formatted. The final version may differ from this version.

pocket and especially in providing the molecular machinery that may be required for the action of receptor ligands. This should be kept in mind when interpreting results from mutational mappings of ligand-receptor interactions in general and in particular for small molecule agonists, as demonstrated for the metal-ion chelator complexes in the present study.

The present agonist tethering and activation mechanism is rather similar to that applied by Buck & Wells using covalent, disulfide tethering (Buck and Wells, 2005) – but with opposite orientation of the attachment site and the second-site interaction point (Fig. 8B). In an elegant study they made small thiol-reactive compounds act as agonists for the C5a receptor by tethering them to a Cys residue introduced at position VI:20 ($Gly^{262}Cys$). From this site the compounds established second-site interactions with an Ile residue located at position III:08 (Ile^{116}), i.e. one helical turn "below" the metal-ion anchor-point, HisIII:05 (Buck and Wells, 2005). Importantly, space-generating mutations at position III:08 increased potency and agonism for the CysVI:20 tethered ligands whereas space-filling, steric hindrance mutagenesis at position III:08 decreased affinity and turned compounds into antagonists (Buck and Wells, 2005). These observations support the notion that agonism is associated with movement of the extracellular segments of TM-VI and TM-III toward each other.

As illustrated by the CXCR3 receptor in the present study, the opposing faces of the involved helices often provide much of the molecular equipment required for the stabilization of the active conformation – in this case, three of the four components of the "aromatic zipper". Importantly however, the CXCR3 receptor does not display any sign of ligand independent or constitutive signaling efficacy. Thus, the interaction of the three aromatic residues: PheIII:08, TyrVI:16, and TyrVII:10 is apparently not strong enough in the CXCR3 receptor to hold the receptor in its active conformation and thereby leading

Molecular Pharmacology Fast Forward. Published on December 14, 2006 as DOI: 10.1124/mol.106.030031
This article has not been copyedited and formatted. The final version may differ from this version.

to ligand-independent signaling. However, in for example the ghrelin receptor, a similar aromatic cluster on the opposing faces of TM-VI and VII - comprising PheVI:16, PheVII:06 and PheVII:09 - is essential for the ~ 50 % constitutive signaling activity of this receptor (Holst *et al.*, 2004). Interestingly, naturally occurring mutations in the aromatic cluster (PheVI:16) selectively eliminates the constitutive activity of this receptor and leads to a clinical syndrome characterized by short stature and obesity (Pantel et al., 2006;Holst and Schwartz, 2006).

Large molecule agonists

Many agonists for 7TM receptors are large molecules such as peptide hormones and chemokines, which are known to interact mainly with the N-terminal extension, the loop regions, and perhaps the extracellular ends of the helices (Schwartz and Holst, 2002;Vassart et al., 2004;Schwarz and Wells, 2002). It is interesting to note, that the metal-ion site-engineered CXCR3 receptor can be activated by both the large endogenous chemokine agonists and by the small metal-ion chelator complexes. Importantly, the three aromatic residues from TM-III, -VI and –VII, which interdigitate to form the “aromatic zipper” deep in the pocket are only essential for the agonist activity of the small molecule chelators and not at all for the large chemokine proteins (Table 2). Previously we have found that a metal-ion site-engineered NK1 receptor can be activated both by Zn(II) ions binding between positions III:08 and VII:06 and by the endogenous substance P neuropeptide acting at exterior epitopes (Holst *et al.*, 1998;Holst *et al.*, 2000). In that case, steric hindrance mutagenesis demonstrated that substance P does not reach deep down in the main ligand binding pocket to act as an agonist (Holst *et al.*, 1998). It is proposed that large agonists such as chemokines, peptide hormones and neuropeptides act as agonists by stabilizing a similar active conformation as presented in the present study for the small molecule aromatic

Molecular Pharmacology Fast Forward. Published on December 14, 2006 as DOI: 10.1124/mol.106.030031
This article has not been copyedited and formatted. The final version may differ from this version.

chelators; but, that they do so by acting in a “Velcro-like” manner involving binding to multiple, more extracellular epitopes of the receptor. Such large agonists may or may not - in addition - interact with residues in the main ligand binding pocket. But, that is not required. There does not appear to be a common “lock” for all the different agonist “keys” in 7TM receptor; but, there probably is a common molecular activation mechanism (Schwartz and Rosenkilde, 1996). That is, the chemically highly diverse agonists are expected to stabilize similar active receptor conformations in their respective target receptors through binding in rather significantly different manners at different sites, depending on their size and chemical properties of the agonists (Elling *et al.*, 2006).

Alternative models for CXCR3 receptor activation

The results of the present study has above been discussed in relation to the Global Toggle Switch model for 7TM receptor activation in which a large degree of induced fit is part of the ligand binding but where the activation mechanism is believed to be a result of a concerted action type of allostery (Elling et al., 2006;Schwartz et al., 2006). An alternative sequential type of allosteric model for 7TM activation has been advocated especially by Pardo and coworkers (Urizar et al., 2005;Jongejan et al., 2005). This model does not involve major conformational changes of the helical segments around the main ligand binding crevice, but instead it requires that the agonist touches key residues, which through a “domino effect” from residue to residue down through the helical bundle eventually releases the major conformational changes occurring at the intracellular face of the receptor. Key residues in this model are residues III:12 (3.36), VII:12 (7.45), VI:13 (6.48); VII:16 (7.49), II:10 (2.50), and III:26 (3.50) (Urizar et al., 2005;Jongejan et al., 2005). We agree that these and other more-or-less conserved residues will change, for example, rotamer states and/or hydrogen bond partners during

Molecular Pharmacology Fast Forward. Published on December 14, 2006 as DOI: 10.1124/mol.106.030031
This article has not been copyedited and formatted. The final version may differ from this version.

receptor activation. But, we consider these conformational changes to be part of the concerted Global Toggle Switch mechanism. Nevertheless, in the case of the bipyridine agonist, it could in principle act solely by touching PheIII:12, which is located at the bottom of the proposed binding pocket - corresponding to SerIII:12 in the histidine H1 receptor (Jongejan et al., 2005). However, it should be noted that when PheIII:12 was mutated as part of the search for second-site interactions in the CXCR3 receptor, very little effect was observed on the agonism of, for example, bipyridine (Table 2). However, the present study was not designed to try to differentiate between the two models for receptor activation. Recently a novel X-ray structure of a presumed active form of rhodopsin was presented in which minimal changes of the helical bundle had occurred (Salom et al., 2006). This does not fit with neither of the above discussed models which both incorporates major conformational changes of at least the intracellular helical segments (Hubbell et al., 2003).

Design and development of non-peptide agonists for 7TM receptors.

In relation to drug discovery, the observation that it is possible to make a small, simple ligand such as bipyridine act as an efficient agonist – even a super-agonist - for a receptor, which normally is activated by a large chemokine protein is notable. Especially because this is achieved simply by ensuring that the small ligand through a single point mutation is tethered at the right position in the main ligand-binding pocket. This indicates, that it should be possible to design and develop small molecule agonists for 7TM receptors in general, i.e. based on knowledge of the physicochemical properties of the binding pocket - importantly, the binding pocket presented in the *active* receptor conformation.

Molecular Pharmacology Fast Forward. Published on December 14, 2006 as DOI: 10.1124/mol.106.030031
This article has not been copyedited and formatted. The final version may differ from this version.

ACKNOWLEDGEMENTS

Lisbet Elbak and Inger Smith Simonsen are thanked for excellent technical help throughout this study.

REFERENCES

Ballesteros JA, Jensen A D, Liapakis G, Rasmussen S G, Shi L, Gether U and Javitch J A (2001) Activation of the Beta 2-Adrenergic Receptor Involves Disruption of an Ionic Lock Between the Cytoplasmic Ends of Transmembrane Segments 3 and 6. *J Biol Chem* **276**:29171-29177.

Berridge MJ, Dawson M C, Downes C P, Heslop J P and Irvin R F (1983) Changes in the Level of Inositol Phosphates After Agonist-Dependent Hydrolysis of Membrane Phosphoinositides. *Biochem J* **212**:473-482.

Bockaert J and Pin J P (1999) Molecular Tinkering of G Protein-Coupled Receptors: an Evolutionary Success. *EMBO J* **18**:1723-1729.

Buck E and Wells J A (2005) Disulfide Trapping to Localize Small-Molecule Agonists and Antagonists for a G Protein-Coupled Receptor. *Proc Natl Acad Sci U S A* **102**:2719-2724.

Carmine R.D., Molinari P, Sbraccia M, Ambrosio C and Costa T (2004) "Induced-Fit" Mechanism for Catecholamine Binding to the Beta2-Adrenergic Receptor. *Mol Pharmacol* **66**:356-363.

Elling CE, Frimurer T M, Gerlach L O, Jorgensen R, Holst B and Schwartz T W (2006) Metal-Ion Site Engineering Indicating a Global Toggle Switch Model for 7TM Receptor Activation. *J Biol Chem* **281**:17337-17343.

Farrens DL, Altenbach C, Yang K, Hubbell W L and Khorana H G (1996) Requirement of Rigid-Body Motion of Transmembrane Helices for Light Activation of Rhodopsin. *Science* **274**:768-770.

Gerlach LO, Jakobsen J S, Jensen K P, Rosenkilde M R, Skerlj R T, Ryde U, Bridger G J and Schwartz T W (2003) Metal Ion Enhanced Binding of AMD3100 to Asp262 in the CXCR4 Receptor. *Biochemistry* **42**:710-717.

Gether U, Lin S, Ghanouni P, Ballesteros J A, Weinstein H and Kobilka B K (1997) Agonist Induced Conformational Changes in Transmembrane Domains III and VI of the Beta2 Adrenoceptor. *EMBO J* **16**:6737-6747.

Han SJ, Hamdan F F, Kim S K, Jacobson K A, Bloodworth L M, Li B and Wess J (2005) Identification of an Agonist-Induced Conformational Change Occurring Adjacent to the Ligand-Binding Pocket of the M(3) Muscarinic Acetylcholine Receptor. *J Biol Chem* **280**:34849-34858.

Hendlich M, Bergner A, Gunther J and Klebe G (2003) Relibase: Design and Development of a Database for Comprehensive Analysis of Protein-Ligand Interactions. *J Mol Biol* **326**:607-620.

Holst B, Elling C E and Schwartz T W (2000) Partial Agonism Through a Zinc-Ion Switch Constructed Between Transmembrane Domains III and VII in the Tachykinin NK(1) Receptor. *Mol Pharmacol* **58**:263-270.

Holst B, Holliday N D, Bach A, Elling C E, Cox H M and Schwartz T W (2004) Common Structural Basis for Constitutive Activity of the Ghrelin Receptor Family. *J Biol Chem* **279**:53806-53817.

Holst B and Schwartz T W (2006) Ghrelin Receptor Mutations--Too Little Height and Too Much Hunger. *J Clin Invest* **116**:637-641.

Holst B, Zoffmann S, Elling C E, Hjorth S A and Schwartz T W (1998) Steric Hindrance Mutagenesis Versus Alanine Scan in Mapping of Ligand Binding Sites in the Tachykinin NK1 Receptor. *Mol Pharm* **53**:166-175.

Hubbell WL, Altenbach C, Hubbell C M and Khorana H G (2003) Rhodopsin Structure, Dynamics, and Activation: a Perspective From Crystallography, Site-Directed Spin Labeling, Sulfhydryl Reactivity, and Disulfide Cross-Linking. *Adv Protein Chem* **63**:243-290.

Jongejan A, Bruysters M, Ballesteros J A, Haaksma E, Bakker R A, Pardo L and Leurs R (2005) Linking Agonist Binding to Histamine H1 Receptor Activation. *Nat Chem Biol* **1**:98-103.

Kobilka B (2004) Agonist Binding: a Multistep Process. *Mol Pharmacol* **65**:1060-1062.

Kostenis E, Zeng F Y and Wess J (1998) Functional Characterization of a Series of Mutant G Protein Alphaq Subunits Displaying Promiscuous Receptor Coupling Properties. *J Biol Chem* **273**:17886-17892.

Lefkowitz RJ (2004) Historical Review: a Brief History and Personal Retrospective of Seven-Transmembrane Receptors. *Trends Pharmacol Sci* **25**:413-422.

Li J, Edwards P C, Burghammer M, Villa C and Schertler G F (2004) Structure of Bovine Rhodopsin in a Trigonal Crystal Form. *J Mol Biol* **343**:1409-1438.

Li Z and Scheraga H A (1987) Monte Carlo-Minimization Approach to the Multiple-Minima Problem in Protein Folding. *Proc Natl Acad Sci U S A* **84**:6611-6615.

Liapakis G, Chan W C, Papadokostaki M and Javitch J A (2004) Synergistic Contributions of the Functional Groups of Epinephrine to Its Affinity and Efficacy at the Beta2 Adrenergic Receptor. *Mol Pharmacol* **65**:1181-1190.

Okada T, Sugihara M, Bondar A N, Elstner M, Entel P and Buss V (2004) The Retinal Conformation and Its Environment in Rhodopsin in Light of a New 2.2 A Crystal Structure. *J Mol Biol* **342**:571-583.

Palczewski K, Kumasaka T, Hori T, Behnke C A, Motoshima H, Fox B A, Le T, I, Teller D C, Okada T, Stenkamp R E, Yamamoto M and Miyano M (2000) Crystal Structure of Rhodopsin: A G Protein-Coupled Receptor. *Science* **289**:739-745.

Pantel J, Legendre M, Cabrol S, Hilal l, Hajaji Y, Morisset S, Nivot S, Vie-Luton M P, Grouselle D, de K M, Kadiri A, Epelbaum J, Le B Y and Amselem S (2006) Loss of Constitutive Activity of the Growth Hormone Secretagogue Receptor in Familial Short Stature. *J Clin Invest* **116**:760-768.

Rosenkilde MM, Gerlach L O, Jakobsen J S, Skerlj R T, Bridger G J and Schwartz T W (2004) Molecular Mechanism of AMD3100 Antagonism in the CXCR4 Receptor: Transfer of Binding Site to the CXCR3 Receptor. *J Biol Chem* **279**:3033-3041.

Rosenkilde MM, Kledal T N, Brauner-Osborne H and Schwartz T W (1999) Agonists and Inverse Agonists for the Herpesvirus 8-Encoded Constitutively Active Seven-Transmembrane Oncogene Product, ORF-74. *J Biol Chem* **274**:956-961.

Ruprecht JJ, Mielke T, Vogel R, Villa C and Schertler G F (2004) Electron Crystallography Reveals the Structure of Metarhodopsin I. *EMBO J* **23**:3609-3620.

Sakmar TP, Menon S T, Marin E P and Awad E S (2002) Rhodopsin: Insights From Recent Structural Studies. *Annu Rev Biophys Biomol Struct* **31**:443-484.

Salom D, Lodowski D T, Stenkamp R E, Trong I L, Golczak M, Jastrzebska B, Harris T, Ballesteros J A and Palczewski K (2006) Crystal Structure of a Photoactivated Deprotonated Intermediate of Rhodopsin. *Proc Natl Acad Sci U S A* **103**:16123-16128.

Schwartz TW, Frimurer T M, Holst B, Rosenkilde M M and Elling C E (2006) Molecular Mechanism of 7TM Receptor Activation - A Global Toggle Switch Model. *Annu Rev Pharmacol Toxicol* **46**:481-519.

Schwartz TW, Gether U, Schambye H T and Hjorth S A (1995) Molecular Mechanism of Action of Non-Peptide Ligands for Peptide Receptors. *Curr Pharmaceut Design* **1**:325-342.

Schwartz TW and Holst B (2006) Ago-Allosteric Modulation and Other Types of Allostery in 7TM Receptors. *J Recept Signal Transduct* **26**:107-128.

Schwartz TW and Holst B (2002) Molecular Structure and Function of 7TM/G-protein Coupled Receptors, in *Textbook of Receptor Pharmacology* (Forman JC and Johansen T eds) pp 65-84, CRC Press, Bocan Rouge, FL.

Schwartz TW and Rosenkilde M M (1996) Is There a 'Lock' for All 'Keys' in 7TM Receptors. *Trends Pharmacol Sci* **17**:213-216.

Schwarz MK and Wells T N (2002) New Therapeutics That Modulate Chemokine Networks. *Nat Rev Drug Discov* **1**:347-358.

Shi L and Javitch J A (2002) The Binding Site of Aminergic G Protein-Coupled Receptors: the Transmembrane Segments and Second Extracellular Loop. *Annu Rev Pharmacol Toxicol* **42**:437-467.

Strader CD, Gaffney T, Sugg E E, Candelore M R, Keys R, Patchett A A and Dixon R A F (1991) Allele-Specific Activation of Genetically Engineered Receptors. *J Biol Chem* **266**:5-8.

Swaminath G, Xiang Y, Lee T W, Steenhuis J, Parnot C and Kobilka B K (2004) Sequential Binding of Agonists to the Beta2 Adrenoceptor. Kinetic Evidence for Intermediate Conformational States. *J Biol Chem* **279**:686-691.

Urizar E, Claeysen S, Deupi X, Govaerts C, Costagliola S, Vassart G and Pardo L (2005) An Activation Switch in the Rhodopsin Family of G Protein-Coupled Receptors: the Thyrotropin Receptor. *J Biol Chem* **280**:17135-17141.

Vassart G, Pardo L and Costagliola S (2004) A Molecular Dissection of the Glycoprotein Hormone Receptors. *Trends Biochem Sci* **29**:119-126.

Wieland K, Zuurmond H M, Krasel C, Ijzerman A P and Lohse M J (1996) Involvement of Asn-293 in Stereospecific Agonist Recognition and in Activation of the Beta2-Adrenergic Receptor. *Proc Natl Acad Sci (USA)* **93**:9276-9281.

Molecular Pharmacology Fast Forward. Published on December 14, 2006 as DOI: 10.1124/mol.106.030031
This article has not been copyedited and formatted. The final version may differ from this version.

FOOTNOTES

This study was supported by grants from the Novo Nordisk Foundation, the Danish Medical Research Council and from the European Community's Sixth Framework Program (grant LSHB-CT-2003-503337 and LSHB-CT-2005-518167).

1. Correspondence should be addressed to either of these persons MMR, TMF or TWS

2. In our model the closest distance between bipyridine and PheIII:08 is ~ 8 Å and TyrVI:17 is located between. It would require major non-favorable alterations to the model – or a whole other molecular model - to bring the bipyridine in direct contact with PheIII:08.

3. The issue, that there will be differences between the molecular mechanism of antagonism and inverse agonism, is not dealt with here because the present paper focuses on agonism.

Molecular Pharmacology Fast Forward. Published on December 14, 2006 as DOI: 10.1124/mol.106.030031
This article has not been copyedited and formatted. The final version may differ from this version.

LEGENDS FOR FIGURES

Fig. 1. The CXCR3 receptor used for metal-ion site engineering and molecular modeling and simulation. *Panel A* – serpentine model of the CXCR3 receptor. In dark red are highlighted the two residues comprising the anchoring metal-ion site: the His introduced in stead of GlyIII:05 (Gly^{128}) and the endogenous AspIV:20 (Asp^{186}). In light red are highlighted various residues which are mutated to try to identify potential metal-ion site partners, second-site interaction sites for the aromatic chelators, or supporting "aromatic zipper" residues (see Figs. 6 and 7). The position of PheIII:08 (Phe^{131}), TyrVI:16 (Tyr^{271}), and TyrVII:10 (Tyr^{308}) are specifically indicated. In grey are highlighted conserved fingerprint residues, which characterize the individual transmembrane segments. *Panel B* - a molecular model of the seven helical bundle of the basic [HisIII:08]-CXCR3 receptor construct built over the X-ray structure of the inactive, dark state of rhodopsin (Palczewski *et al.*, 2000) in blue solid ribbon format. The two residues which according to the Relibase® analysis and molecular modeling can form an ideal metal-ion site in the inactive form of the receptor: HisIII:08 and AspIV:20 are shown in stick models as ligands for a metal-ion (magenta sphere) docked into the receptor model (see text for details).

Fig. 2. Construction of an inter-helical, bi-dentate metal-ion binding site between position III:05 and position IV:20 in the CXCR3 chemokine receptor. *Panel A* - Helical wheel diagram of the CXCR3 receptor as seen from the extracellular side . In grey are highlighted the "fingerprint" residues in each transmembrane helix. It should be noted that this schematic format gives a misleading picture of the actual distances between residues especially between helices (see Fig. 1B). GlyIII:05 was substituted with His (highlighted in red) - as a potential metal-ion binding residue - producing [GlyIII:05His]-CXCR3. Effect of free Cu(II) ions (*Panel B*), the bipyridine chelator (BIP)

Molecular Pharmacology Fast Forward. Published on December 14, 2006 as DOI: 10.1124/mol.106.030031
This article has not been copyedited and formatted. The final version may differ from this version.

alone (*Panel C*), and the Cu-bipyridine metal-ion chelator complex (*Panel D*) on signal transduction as measured by inositol trisphosphate (IP3) accumulation in control cells (△) and in COS-7 cells transiently transfected with either the CXCR3 wild-type (●), the [GlyIII:05His]-CXCR3 construct (■), or mock transfected cells (open triangles). In panels *B* to *D*, total production of IP3 is indicated in fmol/10^5 cells. *Panel E* - Mutational analysis of the endogenous metal-ion site partner for the introduced HisIII:08 in the CXCR3 receptor. AspIV:20 or AspVI:23 were individually substituted by Asn producing [GlyIII:05His;AspIV:20Asn]-CXCR3 (▲) and [GlyIII:05His; AspVI:23Asn] (□). Dose-response curves for Cu(II)-bipyridine stimulation of IP3 production in transiently transfected COS-7 cells are shown. In broken line is indicated the effect in the [GlyIII:05His] background construct and in dotted line in indicated the effect in the wild-type receptor.

Fig. 3. Comparison of the effect of Cu(II)-bipipyridine and ITAC and coadministration of the two agonists in the [GlyIII:05His]-CXCR3 receptor. *Panel A* – IP3 production in response to Cu(II)-bipyridine as percent of the maximal IP3 production observed under stimulation with the endogenous chemokine, ITAC, in the wild-type CXCR3 receptor (●) and in the [GlyIII:05His]-CXCR3 construct (■). The red arrow indicate the effect of the introduction of the His residue at position III:05. *Panel B* - Dose-response curves for Cu(II)-bipyridine in the absence (●) and presence of 1 nM (○), 10 nM (□) and 100 nM (Δ) of ITAC. *Panel C* - Dose-response curves for ITAC in the absence (●) and presence of 10 μM (○), 100 μM (Δ), and 1 mM (□) of Cu(II)-bipyridine. The two agonists were administered simultaneously (n = 3-4).

Fig. 4. Identification of residues involved in second-site interactions and required for the aromatic chelators in complex with metal-ions to act as agonists in the

Molecular Pharmacology Fast Forward. Published on December 14, 2006 as DOI: 10.1124/mol.106.030031
This article has not been copyedited and formatted. The final version may differ from this version.

[GlyIII:05His]-CXCR3 receptor. *Panel A* - Helical wheel diagram of the [GlyIII:05His]-CXCR3 receptor. AspIV:20 and HisIII:05, which are presumed to make an anchoring, inter-helical bi-dentate metal ion site (see Fig. 1) are highlighted in red. Residues, which were mutated in order to identify the second-site interaction for the aromatic chelators in the [GlyIII:05His]-CXCR3 receptor, are highlighted in green, and the residues, which were introduced at the various positions are indicated in orange. *Panels B-E* - Dose-response curves for Cu(II)-bipyridine in selected receptor constructs: *Panel B* - [GlyIII:05His;ArgV:01Ala;-ArgV:05Ala]-CXCR3 (△); *Panel C* - [GlyIII:05His;LysVII:02Ala]-CXCR3 (◇); *Panel D* - [GlyIII:05His;TrpVI:13Ala]-CXCR3 (●); and *Panel E* - [GlyIII:05His;-TyrVI:16Ala]-CXCR3 (■). In each panel are also shown for comparison the dose-response curve for Cu(II)-bipyridine is the CXCR3 wild-type receptor (dotted curve) and in the [GlyIII:05His]-CXCR3 background construct (hatched curve) as determined in transiently transfected COS-7 cells. The red arrow indicates the 37-fold decrease in potency for the Cu(II)-bipyridine as a result of Ala-substitution of TyrVI:16.

Fig. 5. Molecular modeling and simulation of the presumed activation process of the Zn(II)-bipyridine complex in the [GlyIII:05His]-CXCR3 receptor construct by Zn(II)-bipyridine. Panel A - Zn(II) and bipyridine docked into a molecular model of the seven helical bundle of the [GlyIII:05His]-CXCR3 receptor construct built over the X-ray structure of the inactive, dark state of rhodopsin (Palczewski *et al.*, 2000) shown in blue solid ribbon format. The red dotted lines indicate the presumed tetrahedral coordination of the zinc-ion (magenta ball) by the carboxyl group of AspIV:20, the imidazole side-chain of HisIII:05 and by the two nitrogen's of the bipyridine moiety. The molecular model was subjected to Monte Carlo molecular simulation (see supplementary materials for details) during which NOE distance constraints were applied to the Cβ-Cβ distances between positions III:08, VI:16, and VII:06 in the extracellular segments of these helices

Molecular Pharmacology Fast Forward. Published on December 14, 2006 as DOI: 10.1124/mol.106.030031
This article has not been copyedited and formatted. The final version may differ from this version.

in order to try to satisfy the activating metal-ion sites previously constructed in the β2-adrenergic receptor (Elling *et al.*, 2006). Conversely, NOE distance constraints were applied to the intracellular segments of TM-VI relative to TM-III and TM-V as well as TM-VII relative to TM-II and –III to try to account for the movements of these helices during activation of rhodopsin as identified by the EPR analysis (Hubbell *et al.*, 2003). The backbone of TM-I through TM-V was not allowed to move during these molecular simulation experiments. In green ribbons are shown the position of TM-VI and TM-VII in a presumed active conformation after the molecular simulation of the activation process. TyrVI:16 on the inner face of TM-VI, which by the mutagenesis was indicated to be the major second-site interaction point for the metal-ion chelator complexes (Fig. 2), is highlighted. The yellow arrows indicate the proposed inward movement of the extracellular segments of TM-VI and TM-VII, whereas hatched dark arrows indicate the opposite, outward movement of the intracellular segments of these helices. *Panel B* - root mean square deviation (RMSD) between the inactive and the activated CXCR3 receptor conformation measured during the molecular simulation procedure. *Panel C* – in black is shown the distance between the side-chain of TyrVI:16 (aromatic atom CE1) and the lower ring of the bipyridine ligand (atom C11) and in red is shown the distance between the side-chain of TyrVI:16 (aromatic atom CD1) and the phenyl side-chain of PheIII:08 (aromatic atom CD2) (in red) measured throughout the molecular simulation.

Fig. 6. The "aromatic zipper" which is proposed to be responsible for the activation of the [GlyIII:05His]-CXCR3 receptor by Zn(II)-bipyridine. *Panel A* - Top view of the aromatic zipper shown both in the inactive state (green ribbon and red distances) and in the proposed active state at the end of the molecular simulation (green ribbon and green distances – see text for details). The orange arrow indicates the direction of the proposed inward movement of TM-VI through which TyrVI:20 is brought

into a position between the metal-ion site anchored bipyridine moiety and the side chain of PheIII:08 during the activation process. TyrVII:10, which completes the presumed aromatic zipper on the opposite side of PheIII:08, is also shown. *Panel B* - Side view of the aromatic zipper as seen from TM-III, which together with TM-IV, has been omitted except for the side-chain of PheIII:08.

Fig. 7. Mutational characterization of the "aromatic zipper" which according to the molecular simulations is proposed to be generated across the main ligand-binding pocket of the [GlyIII:05His]-CXCR3 receptor through the metal-ion site guided binding of the chelator. *Panel A* - Helical wheel diagram of the [GlyIII:05His]-CXCR3 receptor. AspIV:20 and HisIII:05, which constitute the anchoring, inter-helical metal-ion site (see Fig. 1), are highlighted in red. The aromatic chelator - in this case bipyridine - TyrVI:16 (identified as a second site interaction point for the chelator - see Fig. 2) as well as PheIII:08 and TyrVII:10, which were suggested by the molecular simulation to be supporting parts of the aromatic zipper and consequently were subjected to Ala-substitution, are all highlighted in green. *Panel B* - dose-response curves for Cu(II)-bipyridine (panel *i*), Zn(II)-bipyridine (panel *ii)*, and Cu(II)-phenanthroline (panel *iii*) in respect of stimulation of IP3 turnover in COS-7 cells transiently transfected with the [GlyIII:05His;PheIII:08Ala]-CXCR3 construct (solid symbols). For comparison are shown the dose-response curves for the indicated metal-ion chelator complex in the positive control, i.e. the [GlyIII:05His]-CXCR3 background construct (in open squares) and in the negative control, i.e. the wild-type CXCR3 receptor (open triangles). *Panel C* - dose-response curves for Cu(II)-bipyridine (panel *i*), Zn(II)-bipyridine (panel *ii)*, and Cu(II)-phenanthroline (panel *iii*) in respect of stimulation of IP3 turnover in COS-7 cells transiently transfected with the [GlyIII:05His;

Molecular Pharmacology Fast Forward. Published on December 14, 2006 as DOI: 10.1124/mol.106.030031
This article has not been copyedited and formatted. The final version may differ from this version.

TyrVII:10Ala]-CXCR3 construct (solid symbols) with positive and negative controls as in Panel B.

Fig. 8. Presumed binding site residues and activation mechanism for two tethered small molecule agonists compared to a prototype agonist in 7TM receptors. *Panel A* - interaction residues in the β2-adrenergic receptor for the freely diffusible agonist isoproterenol. In a molecular model of the backbone of the seven helical bundle from the X-ray structure of the dark, inactive state of rhodopsin - shown in solid ribbon format - the position of the presumed agonist binding residues are indicated in red. A stick model of isoproterenol illustrate the spatial gap to the interaction residues in especially TM-VI in accordance with the prevailing induced fit binding models (Carmine R.D. et al., 2004;Kobilka, 2004;Swaminath et al., 2004;Liapakis et al., 2004). Orange arrows indicate the presumed inward movements of the extracellular segments of TM-VI and –VII according to the Global Toggle Switch activation model (Elling *et al.*, 2006). *Panel B* - binding sites for tethered ligands - comparison of the metal-ion site tethering approach of the present study with the disulfide tethering approach of Buck & Wells (Buck and Wells, 2005). Positions IV:20 and III:05 which are used for the metal-ion site tethering of the aromatic chelators as well as position VI:16 identified as the main second-site interaction point are all indicated in red (data from the present study). In green are highlighted position VI:20 used for covalent disulfide tethering of small thiol-reactive compounds, which act as agonists by making second-site interactions with an Ile in position III:08 (also shown in green) (Buck and Wells, 2005). Introduction of a space-filling Trp residue at position III:08 decreased affinity and turned compounds into antagonists, whereas Ala in position III:08 increased affinity and turned compounds into agonists. Thus in both of these cases of relatively well defined, “anchored” ligands as well as in the monoamine case (panel A), the small molecule agonist binds between TM-III, -V, VI, and VII and

Molecular Pharmacology Fast Forward. Published on December 14, 2006 as DOI: 10.1124/mol.106.030031
This article has not been copyedited and formatted. The final version may differ from this version.

apparently act through holding the extracellular segments of TM-VI and-VII in an inwardly bent conformation in agreement with the Global Toggle Switch activation mechanism (Elling *et al.*, 2006).

Table 1. Potencies and efficacies of different metal-ion chelator complexes on wt and His III:05 (His^{128})-CXCR3. The effect of the chemokines ITAC and IP10, the metal-ion chelator complexes, the chelators and the metal-ions were meassured by the PI-turnover experiment in transiently transfected COS-7 cells. (n) refers to the number of experiments, $E_{max.}$ (fmol/10^5 cells) refers the maximum stimulation. $F_{inc.}$ refers to the fold increase in potency for each ligand on His III:05-CXCR3 compared to wt CXCR3. $E_{max.}$ (%) refers to the average specific efficacy of a given ligand where 100% equals the maximal specific ITAC stimuation on His III:05-CXCR3. NE=No detectable E_{max}.

		wt-CXCR3				His III:05 (His^{128})-CXCR3					
		Log EC_{50} ± SEM	EC_{50}	(n)	$E_{max.}$ ± SEM	Log EC_{50} ± SEM	EC_{50}	(n)	$F_{inc.}$	$E_{max.}$ ± SEM	$E_{max.}$
			(nM)		*(fmol/10^5 cells)*		*(nM)*		*(fold)*	*(fmol/10^5 cells)*	*%*
Endogenous chemokines	ITAC (CXCL11)	-8,8 ± 0,08	1,7	(23)	544 ± 67	-7,8 ± 0,09	15	(16)	**0,11**	215 ± 31	100
	IP10 (CXCL10)	-8,0 ± 0,10	11	(21)	407 ± 46	-6,9 ± 0,22	163	(14)	**0,07**	163 ± 32	72
			(uM)				*(uM)*		*(fold)*	*(fmol/10^5 cells)*	%
Metal-ion chelator complexes	Cu(II)-Bip.	*(-3.0 ± 0,09*	*973)**	(19)	NE	-4,7 ± 0,11	22	(18)	**44**	347 ± 32	171
	Zn(II)-Bip.	*(-2.9 ± 0,01*	*1169)**	(9)	NE	-4,3 ± 0,08	53	(15)	**22**	313 ± 33	153
	Cu(II)-Phen.	*(-3.5 ± 0,12*	*302)**	(8)	NE	-5,1 ± 0,04	8,0	(10)	**38**	327 ± 60	161
	Zn(II)-Phen.	*(-3.2 ± 0,18*	*595)**	(6)	NE	-4,7 ± 0,05	21	(8)	**29**	300 ± 53	146
Metal-ions	Cu (II)	<-2	>10000	(4)	NE	<-2	>10000	(6)		NE	NE
	Zn (II)	<-2	>10000	(4)	NE	<-2	>10000	(6)		NE	NE

*The EC_{50} was estimated by a non-linear regression using the sigmoidal dose-response algoritm in "GraphPad Prism" with a constant Hill-coefficient of 1.5 corresponding to the Hill-coefficient of the metal-ion chelator complexes on His III:05 CXCR3.

Table 2. Mutational analysis of residues potentially involved in metal-site or as second site interaction. The effect of CuBip and ITAC were meassured by the PI-turnover experiments in transiently transfected COS-7 cells. (n) refers to the number of experiments. $F_{dec.}$ refers to the decrease in potency for CuBip and ITAC on a given mutation compared to His III:05-CXCR3 (background). $E_{max.}$ (fmol/10^5 cells) refers to the maximal stimulation of each ligand . $E_{max.}$ (%) for Cu(II)Bipyridine refers to the efficacy of Cu(II)Bipyridine compared to ITAC. $E_{max.}$ (%) for ITAC refers to the efficacy on each mutation compared to wt CXCR3. NE=No detectable E_{max}.

		Cu(II)-Bipyridine							ITAC					
		SEM	EC_{50}	(n)	$F_{dec.}$	$E_{max.}$ SEM	% E_{max}	Log EC_{50} SEM	EC_{50}	$F_{dec.}$	(n)	$E_{max.}$ SEM	% E_{max}
			(uM)		*(fold)*	*(fmol/10^5 cells)*	*(%)*		*(nM)*	*(fold)*		*(fmol/10^5 cells)*	*(%)*
III:05 *(Background)*	G128H	-4,7 ± 0,11	22	(18)	**1,0**	347 ± 32	162	-7,8 ± 0,09	15	**1,0**	(16)	215 ± 31	36
III:08	F131A	*(-2.8 ± 0,09*	*1415)**	(4)	**64**	NE	NE	-7,5 ± 0,39	35	**2,4**	(3)	72 ± 10	8
III:12	F135L	-4,3 ± 0,23	55	(3)	**2,5**	247 ± 29	172	-8,1 ± 0,14	8,3	**0,57**	(3)	144 ± 28	22
IV:20	D186N	*(-3.1 ± 0,43*	*885)**	(8)	**40**	NE	NE	-8,0 ± 0,20	9	**0,6**	(8)	67 ± 6,9	7
EC2	H202A	-4,2 ± 0,27	58	(3)	**2,6**	153 ± 4,4	180	-7,8 ± 0,13	17	**1,2**	(3)	85 ± 9,6	11
V:01; V:05	R208A; R212A	-4,9 ± 0,05	12	(4)	**0,22**	236 ± 60	259	-7,8 ± 0,36	15	**1,1**	(4)	91 ± 14	12
V:05	R212H	-4,7 ± 0,05	19	(3)	**0,85**	526 ± 122	227	-7,8 ± 0,03	16	**1,1**	(2)	232 ± 33	39
VI:13	W268A	-4,3 ± 0,08	50	(5)	**2,3**	313 ± 68	460	-7,6 ± 0,18	27	**1,9**	(6)	68 ± 11	7
VI:16	Y271A	*(-3.1 ± 0,21*	*794)**	(4)	**37**	NE	NE	-8,8 ± 0,20	1,7	**0,12**	(3)	43 ± 1,8	2,5
VI:16	Y271L	*(-2.9 ± 0,36*	*1278)**	(4)	**58**	NE	NE	-8,9 ± 0,18	1,3	**0,09**	(4)	50 ± 3,0	3,9
VI:16	Y271N	*(-3.2 ± 0,06*	*693)**	(3)	**31**	NE	NE	-8,3 ± 0,38	5,6	**0,39**	(3)	39 ± 2,9	1,8
VI:16	Y271F	-4,3 ± 0,05	51	(3)	**2,3**	263 ± 34	163	-8,1 ± 0,15	7,6	**0,52**	(3)	161 ± 37	25
VI:16	Y271H	-4,0 ± 0,03	108	(5)	**4,9**	196 ± 29	190	-8,0 ± 0,28	9,6	**0,66**	(5)	103 ± 22	14
VI:23	D278N	-4,3 ± 0,12	55	(6)	**2,5**	195 ± 31	267	-7,9 ± 0,02	13	**0,88**	(6)	73 ± 14	8
VII:02	K300A	-4,7 ± 0,09	20	(4)	**0,90**	151 ± 17	150	-8,4 ± 0,05	4,2	**0,29**	(3)	101 ± 12	14
VII:10	Y308A	*(-3.2 ± 0,45*	*631)*	(3)	**29**	NE	NE	-8,1 ± 0,22	7,4	**0,21**	(3)	83 ± 40	10

*The EC_{50} was estimated by a non-linear regression using the sigmoidal dose-response algoritm in "GraphPad Prism" with a constant Hill-coefficient of 1.5 corresponding to the Hill-coefficient of Cu(II)-Bipyridine on His III:05 CXCR3.

Table 3. Comparison of Cu(II) and Zn(II) in complex with Bipyridine and Cu(II) in complex with Phenanthroline in respect of residues potentially involved in metal-site or as second site interaction. The effect of the metal-chelator complexes were meassured by the PI-turnover experiments in transiently transfected COS-7 cells. (n) refers to the number of experiments. F_{dec}. refers to the decrease in potency for each ligand on a given mutation compared to His III:05-CXCR3 (background).

		Cu(II)-Bipyridine					**Zn(II)-Bipyridine**					**Cu(II)-Phenanthroline**				
		EC_{50}	SEM	Kd	(n)	$F_{dec.}$	EC_{50}	SEM	Kd	(n)	$F_{dec.}$	EC_{50}	SEM	Kd	(n)	$F_{dec.}$
				(uM)		*(fold)*			*(uM)*		*(fold)*			*(nM)*		*(fold)*
III:05 *(Background)*	G128H	-4,7 ± 0,11		22	(18)	**1,0**	-4,3 ± 0,08		53	(15)	**1,0**	-4,7 ± 0,05		21	(8)	**1,0**
III:08	F131A	*(-2.8 ± 0,09*		*1415)**	(4)	**64**	*(-3.0 ± 0,15*		*971)**	(6)	**18**	*(-3.0 ± 0,13*		*989)**	(6)	**47**
IV:20	D186N	*(-3.1 ± 0,43*		*885)**	(8)	**40**	*(-2.9 ± 0,31*		*1240)**	(4)	**24**	*(-3.6 ± 0,14*		*241)**	(4)	**12**
V:01; V:05	R208A; R212A	-4,9 ± 0,04		12	(4)	**0,55**	-4,5 ± 0,08		29	(3)	**0,55**	-5,1 ± 0,15		7,9	(3)	**0,38**
VI:13	W268A	-4,3 ± 0,08		50	(5)	**2,3**	-3,7 ± 0,24		190	(4)	**3,6**	-4,5 ± 0,08		33	(6)	**1,6**
VI:16	Y271A	*(-3.1 ± 0,21*		*812)**	(4)	**37**	*(-2.9 ± 0,27*		*1278)**	(3)	**24**	*(-3.4 ± 0,02*		*433)**	(3)	**21**
VI:23	D278N	-4,3 ± 0,12		55	(6)	**2,5**	-3,7 ± 0,16		212	(3)	**4,0**	-4,5 ± 0,04		35	(4)	**1,7**
VII:02	K300A	-4,7 ± 0,09		20	(4)	**0,90**	-4,3 ± 0,07		45	(3)	**0,86**	-5,1 ± 0,07		7,8	(3)	**0,37**
VII:10	Y308A	*(-3.2 ± 0,45*		*651)**	(3)	**29**	*(-3.2 ± 0,70*		*568)**	(3)	**11**	*(-3.4 ± 0,07*		*400)**	(3)	**19**

*The EC50 was estimated by a non-linear regression using the sigmoidal dose-response algoritm in "GraphPad Prism" with a constant Hill-coefficient of 1.5 corresponding to the Hill-coefficient of the metal-ion chelator complexes on His III:05 CXCR3.

Fig. 1

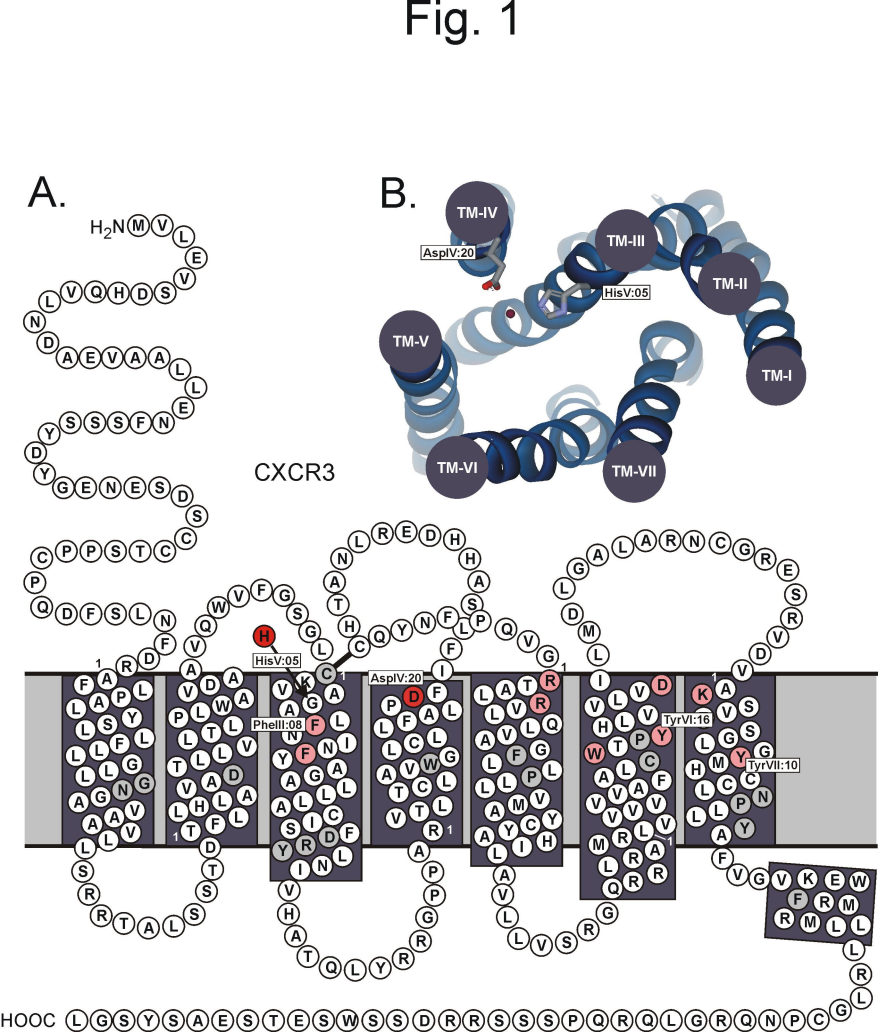
A.
B.
TM-IV
AspIV:20
TM-III
HisV:05
TM-II
TM-V
TM-I
TM-VI
TM-VII
CXCR3
HisV:05
PheIII:08
AspIV:20
TyrVI:16
TyrVII:10
HOOC

Fig. 2

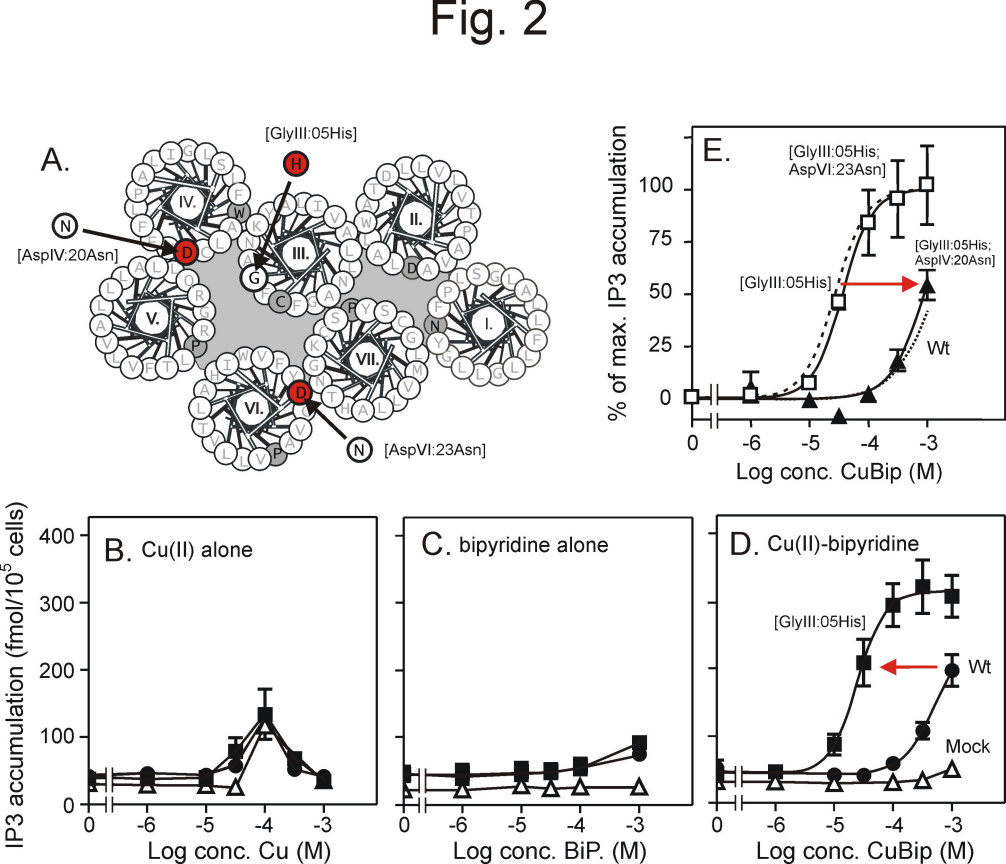
A.
[GlyIII:05His]
[AspIV:20Asn]
[AspVI:23Asn]
I.
II.
III.
IV.
V.
VI.
VII.
E.
[GlyIII:05His; AspVI:23Asn]
[GlyIII:05His; AspIV:20Asn]
[GlyIII:05His]
Wt
% of max. IP3 accumulation
Log conc. CuBip (M)
B. Cu(II) alone
C. bipyridine alone
D. Cu(II)-bipyridine
[GlyIII:05His]
Wt
Mock
IP3 accumulation (fmol/10^5 cells)
Log conc. Cu (M)
Log conc. BiP. (M)
Log conc. CuBip (M)

Fig. 3

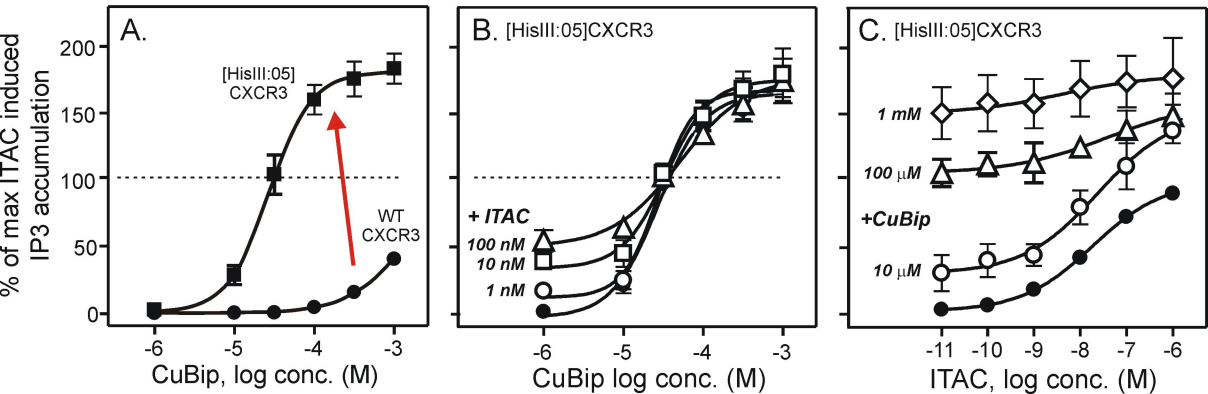
A.
[HisIII:05]
CXCR3
WT
CXCR3
% of max ITAC induced
IP3 accumulation
200
150
100
50
0
-6
-5
-4
-3
CuBip, log conc. (M)
B. [HisIII:05]CXCR3
+ ITAC
100 nM
10 nM
1 nM
-6
-5
-4
-3
CuBip log conc. (M)
C. [HisIII:05]CXCR3
1 mM
100 μM
+CuBip
10 μM
-11
-10
-9
-8
-7
-6
ITAC, log conc. (M)

Fig. 4

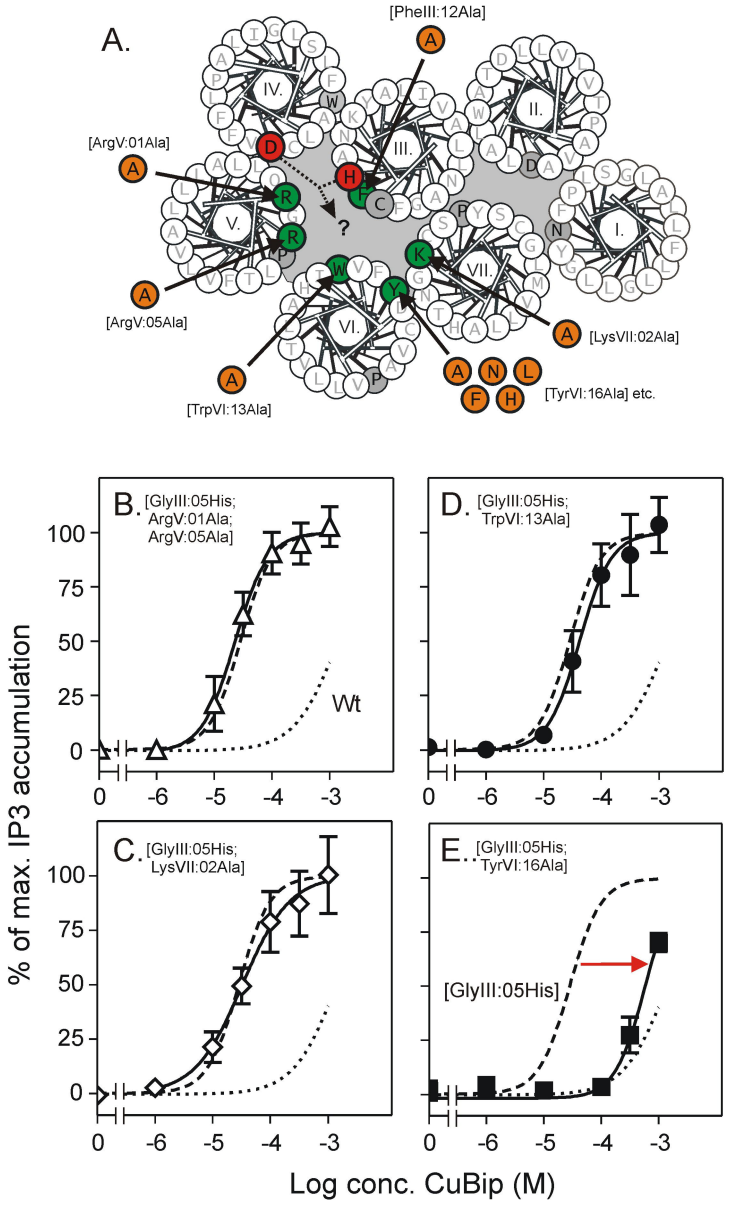
A.
[PheIII:12Ala]
[ArgV:01Ala]
[ArgV:05Ala]
[LysVII:02Ala]
[TrpVI:13Ala]
[TyrVI:16Ala] etc.
IV.
II.
III.
V.
I.
VII.
VI.
B. [GlyIII:05His; ArgV:01Ala; ArgV:05Ala]
Wt
D. [GlyIII:05His; TrpVI:13Ala]
C. [GlyIII:05His; LysVII:02Ala]
E. [GlyIII:05His; TyrVI:16Ala]
[GlyIII:05His]
% of max. IP3 accumulation
Log conc. CuBip (M)

Fig. 5

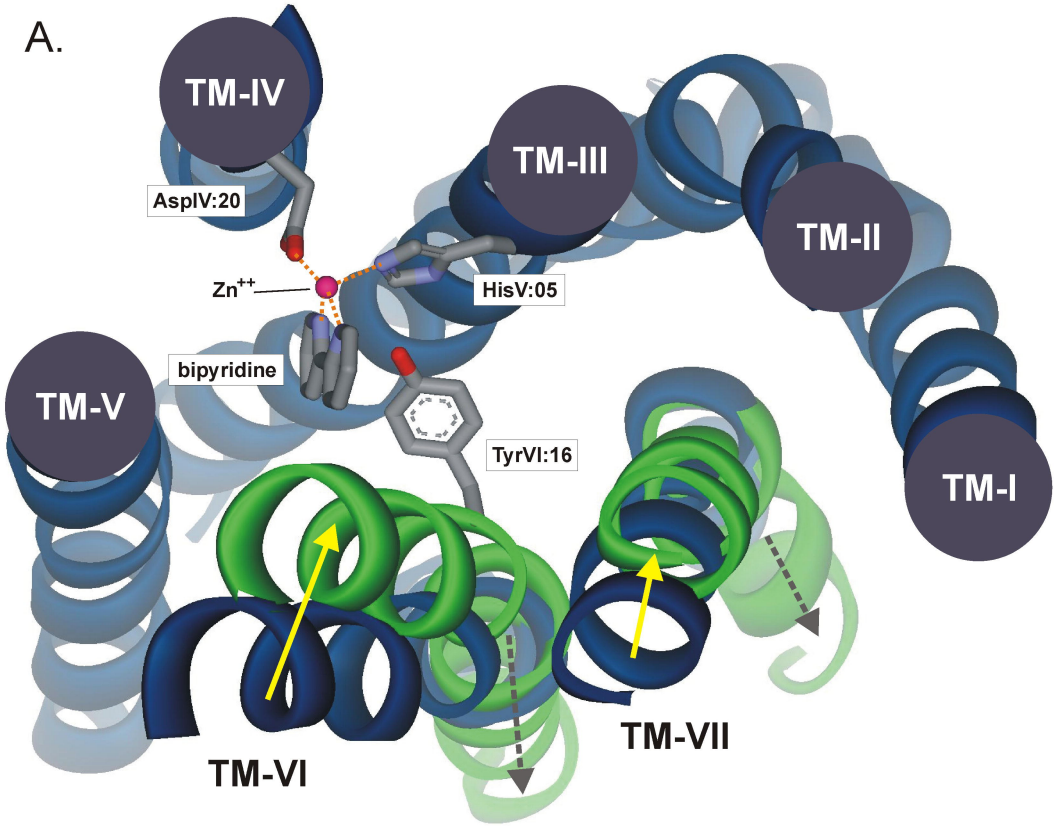
A.
TM-IV
TM-III
TM-II
TM-I
TM-V
TM-VI
TM-VII
AspIV:20
Zn++
HisV:05
bipyridine
TyrVI:16

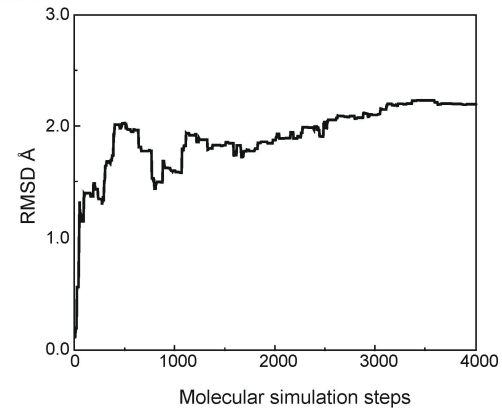
B.
RMSD Å
3.0
2.0
1.0
0.0
0
1000
2000
3000
4000
Molecular simulation steps

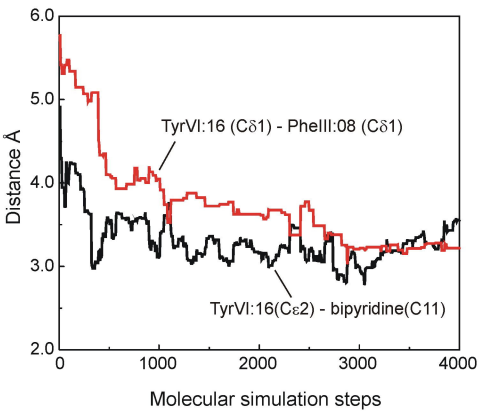
C.
Distance Å
6.0
5.0
4.0
3.0
2.0
TyrVI:16 (Cδ1) - PheIII:08 (Cδ1)
TyrVI:16(Cε2) - bipyridine(C11)
0
1000
2000
3000
4000
Molecular simulation steps

Fig. 6

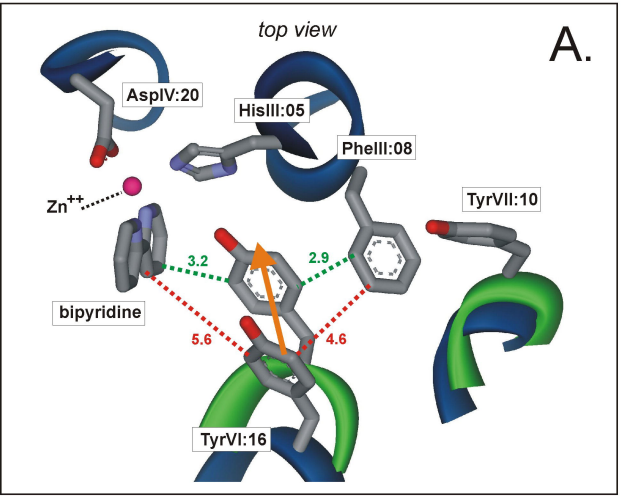
top view
A.
AsplV:20
HisIII:05
PheIII:08
Zn++
TyrVII:10
3.2
2.9
bipyridine
5.6
4.6
TyrVI:16

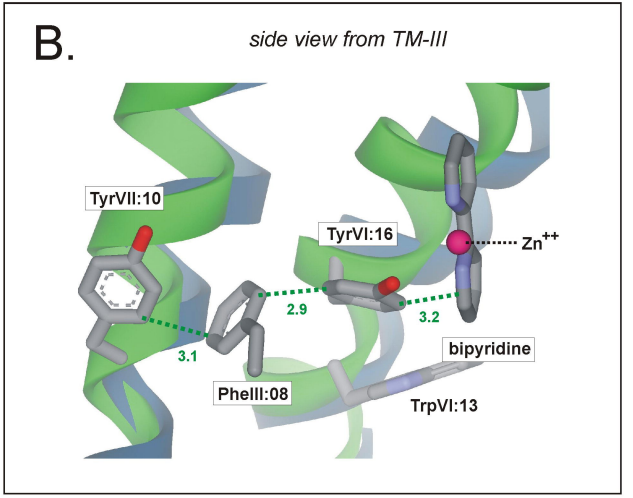
B.
side view from TM-III
TyrVII:10
TyrVI:16
Zn++
2.9
3.2
3.1
bipyridine
PheIII:08
TrpVI:13

Fig. 7

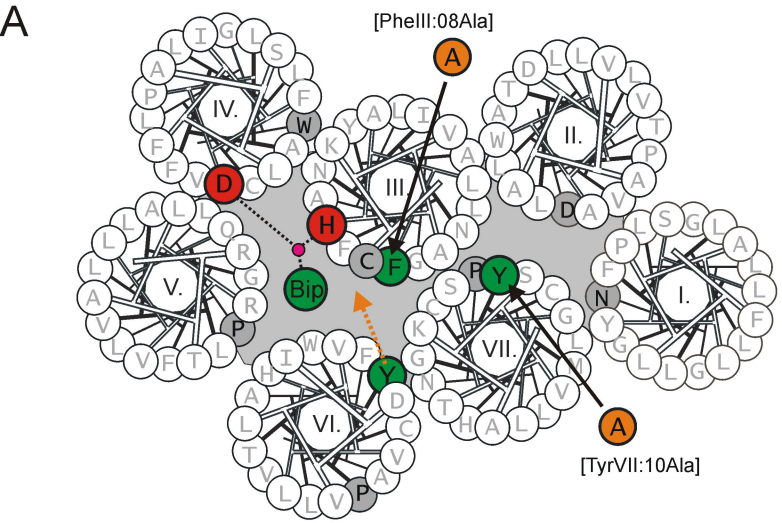
A
[PheIII:08Ala]
A
IV.
II.
III
D
H
C
F
Bip
V.
I.
P
Y
VII.
VI.
A
[TyrVII:10Ala]

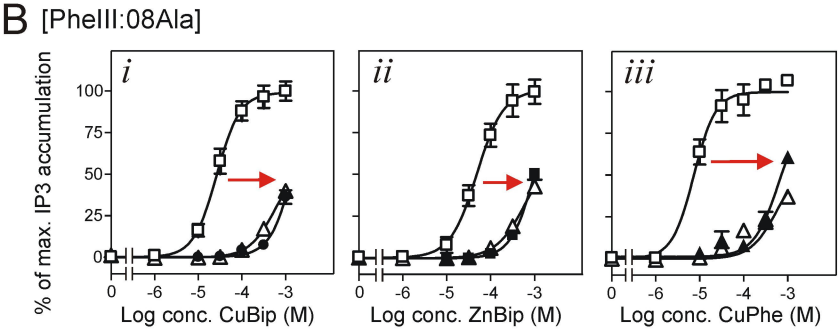
B [PheIII:08Ala]
% of max. IP3 accumulation
i
ii
iii
Log conc. CuBip (M)
Log conc. ZnBip (M)
Log conc. CuPhe (M)

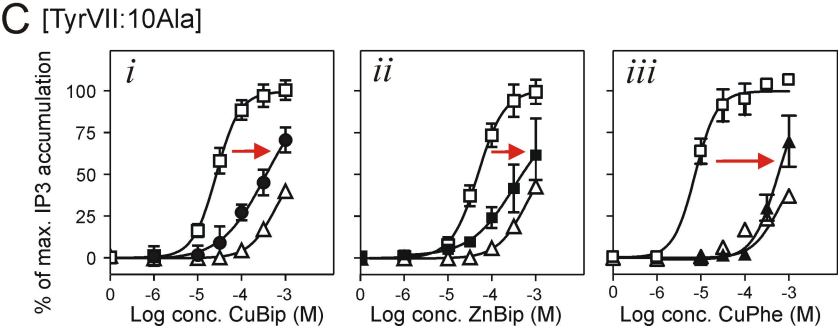
C [TyrVII:10Ala]
% of max. IP3 accumulation
i
ii
iii
Log conc. CuBip (M)
Log conc. ZnBip (M)
Log conc. CuPhe (M)

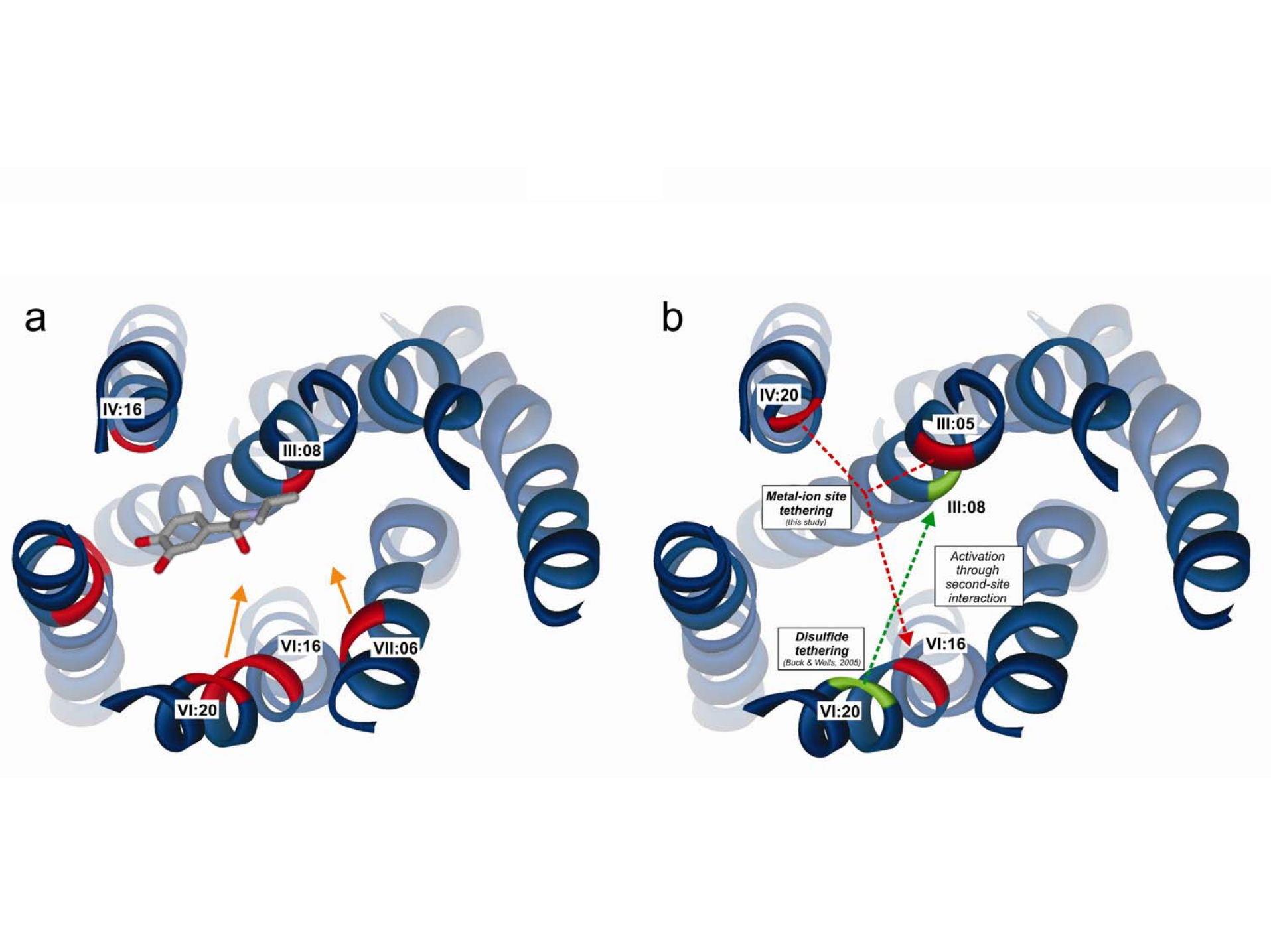
a
IV:16
III:08
VI:16
VII:06
VI:20
b
IV:20
III:05
Metal-ion site tethering
(this study)
III:08
Activation through second-site interaction
Disulfide tethering
(Buck & Wells, 2005)
VI:16
VI:20